Inorg. Chem. **2005**, *44*, 519–528

Structural Variety and Magnetic Properties of Tetranuclear Nickel(II) Complexes with a Central μ_4-Azide

Serhiy Demeshko,[†] Guido Leibeling,[†] Walter Maringgele,[†] Franc Meyer,*[,†] Christopher Mennerich,[‡] Hans-Henning Klauss,[‡] and Hans Pritzkow[||]

Institut für Anorganische Chemie, Georg-August-Universität, Tammannstrasse 4, D-37077 Göttingen, Germany, Institut für Metallphysik und Nukleare Festkörperphysik, TU Braunschweig, Mendelssohnstrasse 3, D-38106 Braunschweig, Germany, and Anorganisch-Chemisches Institut, Universität Heidelberg, Im Neuenheimer Feld 270, D-69120 Heidelberg, Germany

Received June 9, 2004

Using a set of pyrazolate-based dinucleating ligands with thioether sidearms and a set of different carboxylates, seven tetranuclear nickel(II) complexes of types $[L_2Ni_4(N_3)_3(O_2CR)_2](ClO_4)$ (**1**) and $[L_2Ni_4(N_3)(O_2CR)_4](ClO_4)$ (**2**) featuring an unprecedented central μ_4-1,1,3,3-azide could be isolated and fully characterized. X-ray crystal structures are discussed for **1a**,**b**,**e** and **2b**. The μ_4-1,1,3,3-azide is symmetric in all cases except **1a** but exhibits distinct binding modes with significantly different Ni–N_{azide}–Ni angles and Ni–NNN–Ni torsions in type **1** and **2** complexes, which indicates high structural flexibility of this novel bridging unit. Also, IR-spectroscopic signatures and magnetic properties are distinct for type **1** and **2** complexes. Magnetic data for **1a**,**b**,**d**,**e** and **2a**,**b** were investigated and analyzed in a three-*J* approach. The only model that gave a satisfactory fit for all type **1** complexes includes one dominant antiferromagnetic coupling and two ferromagnetic interactions (one large and one smaller), indicating some degree of frustration. On the basis of magneto–structural correlations for *end-on* and *end-to-end* azide linkages, it is reasonable to assign the antiferromagnetic interaction to the *intra*dimer exchange along the pyrazolate and the *end-to-end* linkage of the μ_4-azide. Overall, the magnitude of the coupling constants differs significantly for the two distinct types of compounds, **1** or **2**, and depends on the individual geometric details of the Ni_4 array and the μ_4-1,1,3,3-azide.

Introduction

Stimulated by the growing interest in molecule-based magnetic materials, the past decade has seen extensive research devoted to the study of magnetic interactions between paramagnetic centers in exchange-coupled systems.[1,2] Evolving from the investigation of discrete dinuclear complexes, work in this field has meanwhile developed further. With the objective of obtaining nanoscale molecular magnets, current activities focus on increasing the nuclearity of single-molecule clusters that have ground electronic states with a large spin[3] and enhancing the anisotropy of single-molecule type systems.[4] Nickel(II) is frequently being used in the latter regard due to its large single-ion zero-field splitting. A parallel line of research aims at the synthesis

* Author to whom correspondence should be addressed. E-mail: franc.meyer@chemie.uni-goettingen.de.

[†] Institut für Anorganische Chemie, Georg-August-Universität Göttingen.

[‡] Institut für Metallphysik und Nukleare Festkörperphysik, TU Braunschweig.

[||] Anorganisch-Chemisches Institut, Universität Heidelberg.

(1) (a) Kahn, O. *Angew. Chem.* **1985**, *97*, 837−853; *Angew. Chem., Int. Ed Engl.* **1985**, *24*, 834−850. (b) Kahn, O. *Molecular Magnetism*; VCH: Weinheim, Germany, 1993. (c) Miller, J. S.; Epstein, A. J. *Angew. Chem.* **1994**, *106*, 399−432; *Angew. Chem., Int. Ed. Engl.* **1994**, *33*, 385−388. (d) *Molecule-Based Magnetic Materials*; Turnbull, M. M., Sugimoto, T., Thompson, L. K., Eds.; ACS Symposium Series 644; American Chemical Society: Washington, DC, 1996.

(2) *Magnetism: Molecules to Materials*; Miller, J. S., Drillon, M., Eds.; Wiley-VCH: Weinheim, Germany, 2001.

(3) (a) Sessoli, R.; Tsai, H.-L.; Schake, A. R.; Wang, S.; Vincent, J. B.; Folting, K.; Gatteschi, D.; Christou, G.; Hendrickson, D. N. *J. Am. Chem. Soc.* **1993**, *115*, 1804−1816. (b) Powell, A. K.; Heath, S. L.; Gatteschi, D.; Pardi, L.; Sessoli, R.; Spina, G.; Del Giallo, F.; Pieralli, F. *J. Am. Chem. Soc.* **1995**, *117*, 2491−2502. (c) Müller, A.; Peters, F.; Pope, M. T.; Gatteschi, D. *Chem. Rev.* **1998**, *98*, 239−271. (d) Gatteschi, D.; Sessoli, R.; Cornia, A. *Chem. Commun.* **2000**, 725−732. (e) Larionova, J.; Gross, M.; Pilkington, M.; Andres, H.; Stoeckli-Evans, H.; Güdel, H. U.; Decurtins, S. *Angew. Chem.* **2000**, *112*, 1667−1672; *Angew. Chem., Int. Ed.* **2000**, *39*, 1605−1609.

10.1021/ic049251p CCC: $30.25
Published on Web 01/13/2005

Chart 1. Azide Binding Modes

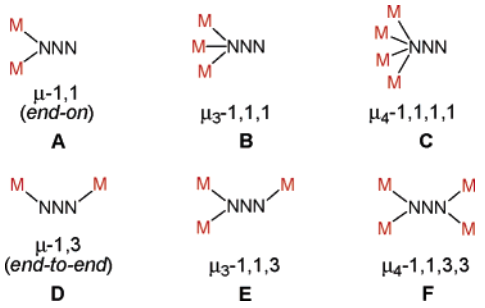

and characterization of materials with molecular architectures extending to one, two, or three dimensions of space and exhibiting long-range magnetic ordering.[2,5,6] For all these intertwined aspects of research within the field of molecule-based magnetism, the flexidentate azido bridge plays a central role, since it mediates different kinds of magnetic coupling depending on its mode of coordination.[7,8] A variety of molecular architectures for azido compounds of different dimensionality have been discovered,[8,9,10] in particular in nickel(II) chemistry (Chart 1).[8,9] Magneto−structural correlations for the two major binding modes of the azido ligand have emerged: those systems featuring μ-1,1 azido bridges (*end-on*, **A**) usually exhibit ferromagnetic (F) coupling, whereas μ-1,3 coordination (*end-to-end*, **D**) entails antiferromagnetic (AF) behavior.[7,8] Only few examples for the triply bridging μ_3-1,1,1 mode **B** are known.[11] Examples for the μ_3-1,1,3 mode **E** (in which both AF and F exchange might occur) are very scarce and have mainly been observed in few 2D- or 3D-polymeric coordination networks where at least one of the M−N distances is very long.[12] Genuine μ_3-1,1,3 azide in some discrete nickel(II) complexes has only recently been reported,[13−15] as have the novel μ_4-1,1,1,1- and μ_4-1,1,3,3-azide binding modes **C** and **F**.[14,16] The more unusual azide binding modes **B**, **C**, **E**, and **F**, however, should be particularly suited for the linking of several metal ions in high-nuclearity clusters and for the construction of 2D and 3D networks of paramagnetic metal centers. This is of major relevance, since magnetic ordering is essentially a three-dimensional property and the design of a molecule-based magnet requires control of the molecular architecture along all three dimensions of space.[17] Hence, there is considerable interest in the exploration of these multiply bridging azide ligands in oligometallic clusters.

We recently communicated the first examples of a novel class of tetranuclear nickel(II) complexes that feature genuine μ_4-1,1,3,3-azide coordination.[14] Molecular structures of two different type **F** complexes revealed a high structural flexibility of such quadruply bridging azides, indicating their potential to act as versatile building blocks in multinuclear complexes. Herein we present a detailed crystallographic and spectroscopic investigation of a whole series of these unique complexes, and we report their magnetic properties and deduce first magneto−structural correlations for the μ_4-azido linkage.

Results and Discussion

Syntheses of Ligands and Complexes. Dinucleating pyrazoles HL^1−HL^4 with thioether sidearms form the basic ligand scaffolds for this work. We previously reported a synthetic route to HL^2, which started from pyrazole-3,5-dicarboxylic acid and proceeded via the corresponding 3,5-

(4) (a) Kahn, O. *Spec. Publ.—R. Soc. Chem.* **2000**, *no. 252*, 150−168 (Metal-Organic and Organic Molecular Magnets). (b) Kahn, O.; Larionova, J.; Ouahab, L. *Chem. Commun.* **1999**, 945−952. (c) Caneschi, A.; Gatteschi, D.; Sangregorio, C.; Sessoli, R.; Sorace, L.; Cornia, A.; Novak, M. A.; Paulsen, C.; Wernsdorfer, W. *J. Magn. Magn. Mater.* **1999**, *200*, 182−201.

(5) Delhaes, P., Drillon, M., Eds.; *Organic and Inorganic Low Dimensional Crystalline Material*; NATO ASI Series, Series B: Physics Vol. 168; Plenum Press: New York, 1987.

(6) See for example: (a) Ferlay, S.; Mallah, T.; Ouahès, R.; Veillet, P.; Verdaguer, M. *Nature* **1995**, *378*, 701−703. (b) Inoue, K.; Hayamizu, T.; Iwamura, H.; Hashizume, D.; Ohashi, Y. *J. Am. Chem. Soc.* **1996**, *118*, 1803−1804. (c) Batten, S. R.; Murray, K. S. *Coord. Chem. Rev.* **2003**, *246*, 103−130.

(7) (a) Charlot, M.-F.; Kahn, O.; Chaillet, M.; Larrieu, C. *J. Am. Chem. Soc.* **1986**, *108*, 2574−2581. (b) Cortés, R.; Lezama, L.; Mautner, F. A.; Rojo, T. In *Molecule-Based Magnetic Materials*; Turnbull, M. M., Sugimoto, T., Thompson, L. K., Eds.; ACS Symposium Series 644; American Chemical Society: Washington, DC, 1996; p 187. (c) Chauduri, P.; Weyhermüller, T.; Bill, E.; Wieghardt, K. *Inorg. Chim. Acta* **1996**, *252*, 195−202. (d) Thompson, L. K.; Tandon, S. S. *Comments Inorg. Chem.* **1996**, *18*, 125−144.

(8) Ribas, J.; Escuer, A.; Monfort, M.; Vicente, R.; Cortés, R.; Lezama, L.; Rojo, T. *Coord. Chem. Rev.* **1999**, *193*−*195*, 1027−1068 and references therein.

(9) Examples for Ni_4 complexes: (a) Ribas, J.; Monfort, M.; Costa, R.; Solans, X. *Inorg. Chem.* **1993**, *32*, 695−699. (b) Serna, Z. E.; Lezama, L.; Urtiaga, M. K.; Arriortua, M. I.; Barandika, M. G.; Cortés, R.; Rojo, T. *Angew. Chem.* **2000**, *112*, 352−355; *Angew. Chem., Int. Ed.* **2000**, *39*, 344−347. (c) Serna, Z. E.; Barandika, M. G.; Cortés, R.; Urtiaga, M. K.; Barberis, G. E.; Rojo, T. *J. Chem. Soc., Dalton Trans.* **2000**, 29−34.

(10) See for example: (a) Escuer, A.; Vicente, R.; El Fallah, M. S.; Goher, M. A.; Mautner, F. A. *Inorg. Chem.* **1998**, *37*, 4466−4469. (b) Abu-Youssef, M. A. M.; Escuer, A.; Goher, M. A. S.; Mautner, F. A.; Reiss, G. J.; Vicente, R. *Angew. Chem.* **2000**, *112*, 1681−1683; *Angew. Chem., Int. Ed.* **2000**, *39*, 1624−1626. (c) Shen, H.-Y.; Bu, W.-M.; Gao, E.-Q.; Liao, D.-Z.; Jiang, Z.-H.; Yan, S.-P.; Wang, G.-L. *Inorg. Chem.* **2000**, *39*, 396−400. (d) Abu-Youssef, M. A.; Drillon, M.; Escuer, A.; Goher, M. A. S.; Mautner, F. A.; Vicente, R. *Inorg. Chem.* **2000**, *39*, 5022−5027.

(11) (a) Halcrow, M. A.; Huffman, J. C.; Christou, G. *Angew. Chem.* **1995**, *107*, 971−973; *Angew. Chem., Int. Ed. Engl.* **1995**, *34*, 4, *889*−*892*. (b) Halcrow, M. A.; Sun, J.-S.; Huffman, J. C.; Christou, G. *Inorg. Chem.* **1995**, *34*, 4167−4177. (c) Wemple, M. W.; Adams, D. M.; Hagen, K. S.; Folting, K.; Hendrickson, D. N.; Christou, G. *Chem. Commun.* **1995**, 1591−1593. (d) Ma, D.; Hikichi, S.; Akita, M.; Moro-oka, Y. *J. Chem. Soc., Dalton Trans.* **2000**, 1123−1134. (e) Goher, M. A. S.; Cano, J.; Journaux, Y.; Abu-Youssef, M. A. M.; Mautner, F. A.; Escuer, A.; Vicente, R. *Chem.—Eur. J.* **2000**, *6*, 778−784.

(12) (a) Monfort, M.; Ribas, J.; Solans, X. *J. Chem. Soc., Chem. Commun.* **1993**, 350−351. (b) Ribas, J.; Monfort, M.; Solans, X.; Drillon, M. *Inorg. Chem.* **1994**, *33*, 742−745. (c) Agrell, I. *Acta Chem. Scand.* **1967**, *21*, 2647−2658. (d) Goher, M. A. S.; Escuer, A.; Abu-Youssef, M. A. M.; Mautner, F. A. *Polyhedron* **1998**, *17*, 4265−4273. (e) Maji, T. K.; Mukherjee, P. S.; Koner, S.; Mostafa, G.; Tuchagues, J.-P.; Chaudhuri, N. R. *Inorg. Chim. Acta* **2001**, *314*, 111−116.

(13) Leibeling, G.; Demeshko, S. Bauer-Siebenlist, B.; Meyer, F.; Pritzkow, H. *Eur. J. Inorg. Chem.* **2004**, 2413−2420.

(14) Meyer, F.; Kircher, P.; Pritzkow, H. *Chem. Commun.* **2003**, 774−775.

(15) Meyer, F.; Demeshko, S.; Leibeling, G.; Kaifer, E.; Pritzkow, H. *Chem.—Eur. J.* **2005**, in press.

(16) (a) Papaefstathiou, G. S.; Perlepes, S. P.; Escuer, A.; Vicente, R.; Font-Bardia, M.; Solans, X. *Angew. Chem.* **2001**, *113*, 908−910; *Angew. Chem., Int. Ed.* **2001**, *40*, 884−886. (b) Papaefstathiou, G. S.; Escuer, A.; Vicente, R.; Font-Bardia, M.; Solans, X.; Perlepes, S. P. *Chem. Commun.* **2001**, 2414−2415.

(17) (a) Kahn, O. *Acc. Chem. Res.* **2000**, *33*, 647−657. (b) Pilkington, M.; Decurtins, S. *Chimia* **2000**, *54*, 593−601.

Scheme 1. Ligand Synthesis

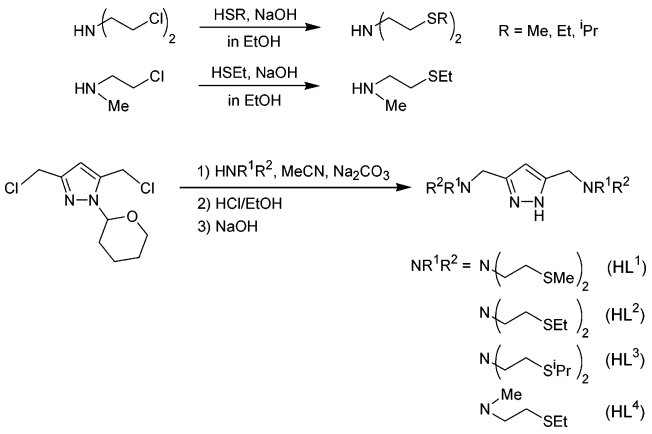

bis(carbamoyl)pyrazole.[18] However, reduction of the latter by $LiAlH_4$ to yield HL^2 proved to be an unreliable step, since cleavage of the sidearm amide bonds occasionally occurred as a minor side reaction, and the resulting one-armed byproducts are difficult to separate. We therefore developed a different synthetic strategy (Scheme 1), which lacks the final reduction step and thus provides purer products. To be able to modify the solubility and crystallization behavior of the resulting complexes, various thioether substituents (Me, Et, ^{i}Pr) have been incorporated. In addition, HL^4 bearing a single thioether arm on each side was prepared by a similar procedure.

Tetranuclear type **1** and **2** complexes are obtained in a straightforward procedure from the appropriate stoichiometric amounts of the respective ligand HL, KO^{t}Bu, $Ni(ClO_4)_2 \cdot 6H_2O$, and NaN_3 and the respective sodium (or potassium) carboxylate. In all complexes, two $\{LNi_2\}$ building units are assembled to give a tetranuclear array that is spanned by a central μ_4-azide (Chart 2). Complexes **1** and **2** differ by the type of additional bridging ligands that hold together the two $\{LNi_2\}$ entities: in the case of compounds **1**, two μ-1,1 azido linkages and two carboxylates are present, while compounds **2** feature four carboxylates. For the latter type **2** compounds, crystalline material could only be obtained with adamantyl carboxylate.

ESI and FAB mass spectrometry proved to be valuable analytical tools to identify the complexes, giving rise to prominent peaks for the monopositive cations $[L_2Ni_4(N_3)_3(O_2CR)_2]^+$ or $[L_2Ni_4(N_3)(O_2CR)_4]^+$, respectively. The FAB mass spectrum of **1e** is shown as an example (Figure 1).

Structural and Spectroscopic Characterization of Complexes. All further discussion will be restricted to those complexes where pure crystalline material could be obtained, since only in these cases a thorough investigation and interpretation of the magnetic properties is possible. Single crystals of **1a**−**e** and **2a**,**b** were analyzed by X-ray crystallography. While the overall constitution was confirmed in all cases, crystallographic data for **1c**,**d** and **2a** are of rather poor quality and will not be described in detail. The molecular structures of the cations of **1b**,**e** and **2b** as well as

(18) Konrad, M.; Meyer, F.; Heinze, K.; Zsolnai, L. *J. Chem. Soc., Dalton Trans.* **1998**, 199−205.

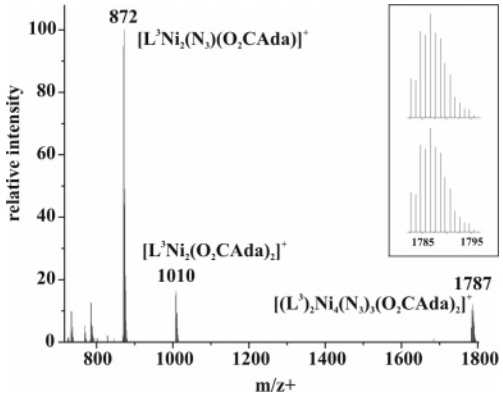

Figure 1. Positive ion FAB mass spectrum of **1e**. The inset shows the experimental (top) and expected (bottom) isotopic distribution patterns for $[(L^3)_2Ni_4(N_3)_3(O_2CAda)_2]^+$.

Chart 2. Complexes

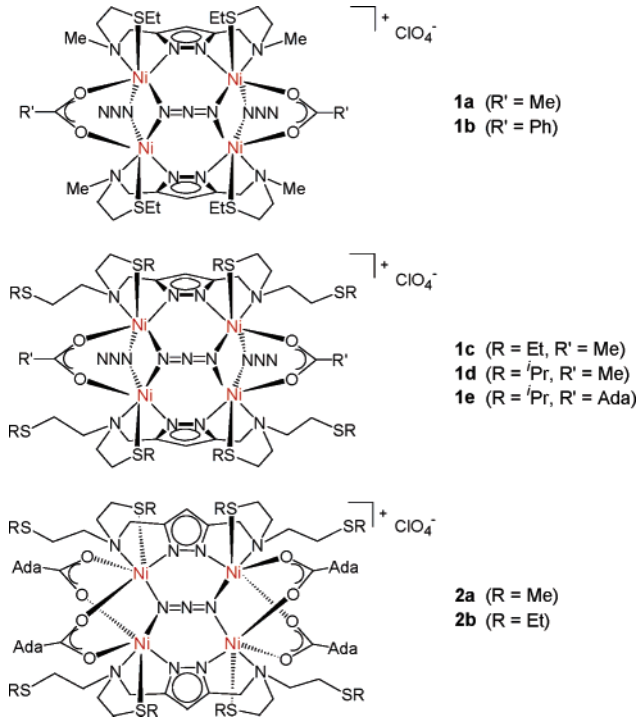

their central tetranuclear cores are depicted as examples in Figures 2−4; selected atom distances and bond angles are collected in Table 1.

Since the pyrazolate ligand generally acts as a bis(tridentate) dinucleating scaffold, some of the thioether sidearms remain uncoordinated and dangling in all cases but those incorporating $[L^4]^-$. All nickel ions are found six-coordinate in distorted octahedral $\{N_4OS\}$ (type **1**) or $\{N_3O_2S\}$ (type **2**) environment. The dinucleating ligand scaffolds enforce a Ni···Ni distance of around 4.5 Å for the metal ions spanned by the pyrazolate. However, Ni···Ni distances for the shorter edges of the Ni_4 array differ significantly, being around 3.15 Å for type **1** complexes with mixed μ-1,1-azido/carboxylate bridges but almost 3.6 Å for type **2** complexes with double carboxylate bridges. This has significant consequences for the overall geometry of the tetranuclear framework and the binding situation for the

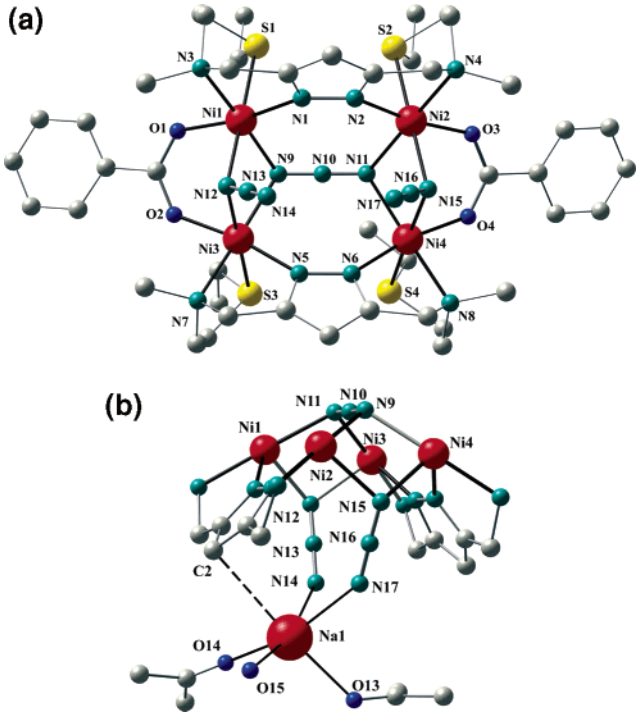

Figure 2. (a) Molecular structure of the cation of **1b**. In the interest of clarity, all hydrogen atoms have been omitted. (b) View of the central core of **1b**, including the sodium ion of cocrystallized $NaClO_4$. Selected atom distances (Å): Na1−O14 2.290(2), Na1−O15 2.335(3), Na1−O13 2.389(2), Na1−N17 2.570(3), Na1−N14 2.543(3), Na1−C2 2.994(3).

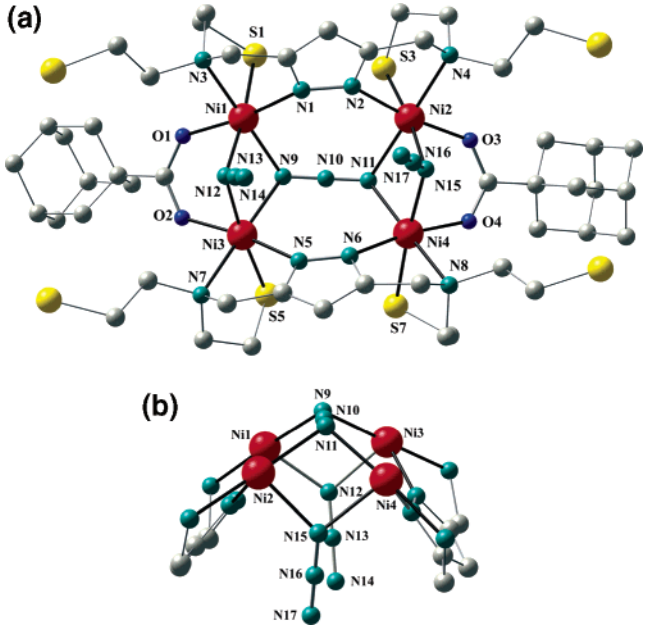

Figure 3. (a) Molecular structure of the cation of **1e**. In the interest of clarity, all hydrogen atoms and the S-bound isopropyl groups have been omitted. (b) View of the central tetranuclear core of **1e**.

central μ_4-azide, since the μ-1,1 linkage of the μ-1,1,3,3-azide has to adapt to these different Ni···Ni distances. In type **1** systems, the μ-1,1,3,3-azide does not fit into the plane of the four Ni ions but caps the Ni_4 rectangle; that is, the Ni−N_3−Ni entities are almost planar with respect to the *end-to-end* linkages (torsion angles Ni1−N9−N11−Ni2 and Ni3−N9−N11−Ni4 are <8.9° for **1a**, <5.5° for **1b**, and <9° for **1e**). In contrast, in type **2** complexes it is the *end-on* bridged Ni ions that are in plane with the central μ_4-azide, while the rectangle of four Ni ions becomes severely distorted with a torsion angle between the Ni1/N9/Ni3 and Ni2/N11/Ni4 planes of ∼53°. This goes along with more acute angles Ni1−N9−Ni3/Ni2−N11−Ni4 in the case of type **1** complexes (91−93°), in contrast to a more open angle of 124° for **2b**. Also, the Ni−N_{azide} bond lengths involving the central μ_4-azide differ significantly: they are found in the range 2.144−2.207(3) Å for type **1** complexes **1a**,**b**,**e**

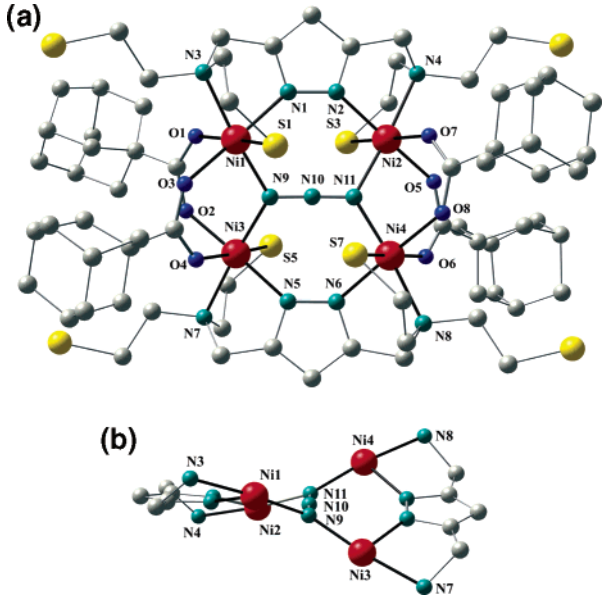

Figure 4. (a) Molecular structure of the cation of **2b**. In the interest of clarity, all hydrogen atoms and the S-bound ethyl groups have been omitted. (b) View of the central tetranuclear core of **2b**.

Table 1. Selected Atom Distances (Å) and Bond Angles (deg) for Complexes **1a,b,e** and **2b**

	1a[a]	1b	1e	2b
Ni1−N1	2.070(4)	2.048(2)	2.039(2)	2.072(5)
Ni1−N9	2.158(4)	2.174(2)	2.162(2)	2.023(5)
Ni1−N12	2.096(4)	2.124(2)	2.126(3)	
Ni2−N2	2.054(4)	2.039(2)	2.070(2)	2.067(5)
Ni2−N11	2.162(4)	2.172(2)	2.204(3)	2.034(5)
Ni2−N15	2.096(4)	2.110(2)	2.086(2)	
Ni3−N5	2.049(5)	2.039(2)	2.059(2)	2.058(5)
Ni3−N9	2.159(4)	2.167(2)	2.203(3)	2.021(5)
Ni3−N12	2.096(4)	2.119(2)	2.100(3)	
Ni4−N6	2.047(4)	2.042(2)	2.046(2)	2.067(5)
Ni4−N11	2.152(5)	2.207(2)	2.161(2)	2.022(5)
Ni4−N15	2.094(4)	2.105(2)	2.121(3)	
N9−N10	1.159(6)	1.179(3)	1.173(3)	1.172(7)
N10−N11	1.195(6)	1.176(3)	1.172(3)	1.161(7)
N12−N13	1.212(6)	1.208(3)	1.192(4)	
N13−N14	1.162(7)	1.152(3)	1.139(5)	
N15−N16	1.192(7)	1.207(3)	1.194(4)	
N16−N17	1.159(8)	1.153(3)	1.147(5)	
Ni1···Ni2	4.525(1)	4.452(1)	4.502(1)	4.521(1)
Ni1···Ni3	3.151(1)	3.146(1)	3.162(1)	3.577(1)
Ni1···Ni4	5.482(1)	5.487(1)	5.440(1)	5.299(1)
Ni2···Ni3	5.494(1)	5.407(1)	5.532(1)	5.310(1)
Ni2···Ni4	3.138(1)	3.123(1)	3.138(1)	3.583(1)
Ni3···Ni4	4.477(1)	4.459(1)	4.492(1)	4.508(1)
Ni1−N9−Ni3	93.7(2)	92.9(1)	92.8(1)	124.4(2)
Ni1−N12−Ni3	97.5(2)	95.7(1)	96.9(1)	
Ni2−N11−Ni4	93.3(2)	91.0(1)	91.9(1)	124.1(2)
Ni2−N15−Ni4	97.0(2)	95.6(1)	96.5(1)	

[a] Values for only one of the two independent (but similar) molecules are listed.

Table 2. Selected IR Absorptions of All New Complexes in cm^{-1}

complex	$\nu_{as}(N_3)$
1a	2081 (vs), 2070 (vs), 2052 (s)
1b	2080 (vs), 2073 (vs), 2044 (s)
1c	2079 (vs), 2074 (vs), 2043 (m)
1d	2082 (vs), 2073 (vs), 2044 (m)
1e	2081 (vs), 2072 (vs), 2045 (m)
2a	2128 (s)
2b	2127 (s)

but are much shorter at 2.021−2.034(5) Å for **2b**. Ni−N_{azide} bond lengths for the μ-1,1-azido ligands in type **1** compounds lie in the intermediate range 2.086−2.126(3) Å. Apparently, the μ_4-bridging azide exhibits considerable structural flexibility and may adapt to various geometric constraints that result from different arrangements of the four metal ions.

Metric parameters of the μ_4-azide itself are very similar in most of the type **1** and **2** complexes. In all cases, the μ_4-azide is almost linear (∼178.5°), and in all cases except **1a** it is symmetric with the N−N bonds in the narrow range 1.172−1.179(3) Å for complexes **1b**,**d**,**e** or 1.161(7)/1.172(7) Å for **2b**. Complex **1a** is a special case, since its central μ_4-azide displays two different N−N bond lengths of 1.156(6)/1.159(6) Å and 1.194(6)/1.195(6) Å. (Two crystallographically independent molecuels are present per unit cell, and bond alternance is observed for both.) Interestingly, the corresponding Ni−N_{azide} distances are not markedly different for the two ends of the N_3 unit. The reason for this asymmetry of the μ_4-azide in **1a** is unclear, but it should be noted that also the azide stretching region of the IR spectrum is slightly distinct for **1a** compared to all other type **1** complexes (see below; Table 2). The bond lengths for the unique μ_4-azide in **1a** are more characteristic for typical μ-1,1-azido ligands, which in all cases (**1a**,**b**,**e**) are highly asymmetric with one long (1.192−1.212(7) Å) and one short (1.139−1.162(7) Å) N−N bond. In the case of **1b**, the latter is slightly lengthened due to the binding of the terminal azide-N to an additional Na^+ ion stemming from cocrystallized $NaClO_4$ (Figure 2b). The Na^+ is located close to the bowl formed by the two pyrazolates and the two μ-1,1-azides and is ligated by the two terminal azide-N, two acetone-O, and one water molecule, with some additional π-interaction to one of the pyrazolate rings (d(Na1−C2) = 2.994(3)). π-interactions of pyrazolate rings with alkali metal ions have been recognized in several cases recently.[19]

While the binding of Na^+ to the μ-1,1-azides in **1b** has no significant effect on the $\nu_{as}(N_3)$ stretches, IR spectroscopy is a valuable tool for distinguishing between type **1** and type **2** complexes (Table 2). The former show three bands at ∼2080, ∼2073, and ∼2044 cm^{-1} (the two high-energy bands are not fully separated in some cases), while the latter display a single major band at ∼2127 cm^{-1} (two additional weak broad bands at ∼2054 and ∼2043 cm^{-1} may possibly be assigned to overtones of the strong perchlorate absorptions at ∼1100 cm^{-1}). Only in the special case of **1a** is the band at lowest frequency slightly shifted compared to all other type **1** complexes (by ∼8 cm^{-1}) and is observed at 2052 cm^{-1}, which might reflect the unique asymmetry of its central μ_4-azide.

(19) (a) Hu, Z.; Gorun, S. M. *Inorg. Chem.* **2001**, *40*, 667−671. (b) Röder, J. C.; Meyer, F.; Kaifer, E.; *Angew. Chem.* **2002**, *114*, 2414−2417; *Angew. Chem. Int. Ed.* **2002**, *41*, 2304−2306.

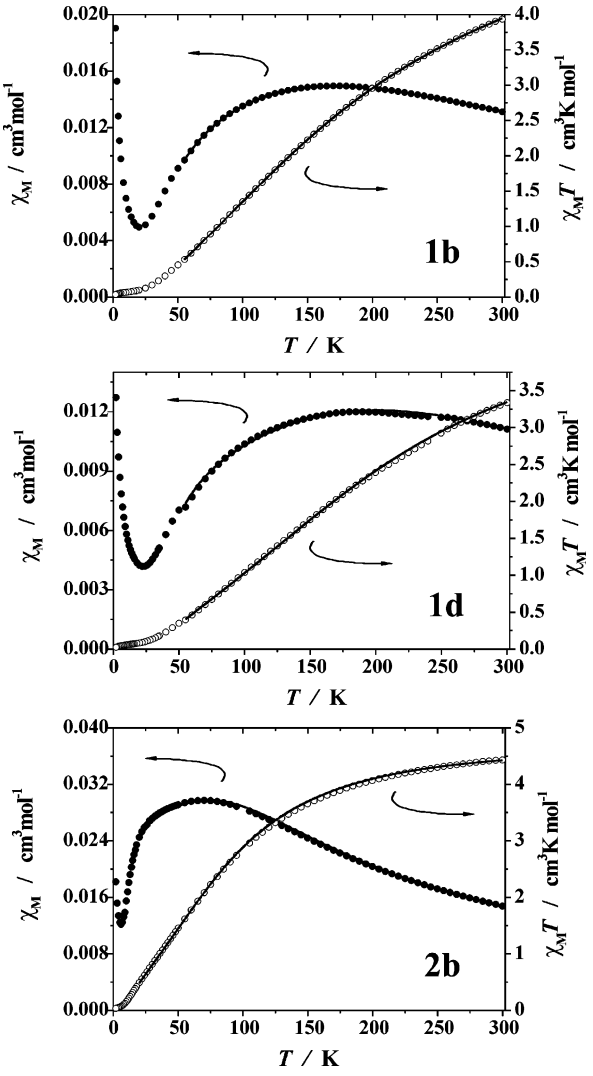

Figure 5. χ_M (solid circles) and $\chi_M T$ (open circles) vs T plot for **1b** (top), **1d** (middle), and **2b** (bottom) at 5000 G. The solid lines represent the fits using the model described in the text.

Magnetic Properties. Magnetic susceptibility measurements for all complexes were carried out at two different magnetic fields (2000 and 5000 G) in the temperature range from 2.0 to 300 K. No significant field dependence was observed. The temperature dependence of the magnetic susceptibility χ_M and the product $\chi_M T$ at 5000 G for complexes **1b**,**d**, and **2b** are shown in Figure 5 as examples.

For all type **1** complexes, the $\chi_M T$ values observed at room temperature are in the range 3.3−3.9 cm^3 K mol^{-1}, that is, much lower than the value expected for four uncoupled nickel(II) ions (4.62 cm^3 K mol^{-1} for g = 2.15), indicating significant antiferromagnetic coupling within the Ni_4 core. Upon cooling, the magnetic susceptibility exhibits a broad maximum at ∼170 K (except in the case of **1c**) while the magnetic moment gradually decreases and tends toward zero at very low temperatures, in accordance with dominant antiferromagnetic exchange and an S = 0 ground state. $\chi_M T$ values for type **2** complexes likewise tend toward zero at

Scheme 2. Magnetic Coupling Model for All New Complexes

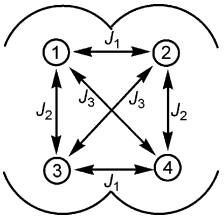

low temperature, but antiferromagnetic coupling is not as strong as in type **1** complexes, which is evidenced by the shift of the broad maximum in the magnetic susceptibility to lower temperatures (~50 K). An increase of χ_M at very low temperatures is probably due to some small amount of residual paramagnetic impurity.

As a simplifying approximation for magnetic data analysis, we assume 2-fold symmetry of the Ni_4 skeleton. Considering the molecular topology of the complexes, we can then expect three principal magnetic exchange pathways according to Scheme 2, comprising one *intra*dimer coupling via the pyrazolate and the *end-to-end* linkage of the central μ_4-1,1,3,3-azide (J_1) and two *inter*dimer couplings along the short edge (J_2) and along the diagonal (J_3) of the Ni_4 rectangle, respectively. The appropriate model is based on the isotropic exchange Hamiltonian $\hat{H}_J = -J_1(S_1S_2 + S_3S_4) - J_2(S_1S_3 + S_2S_4) - J_3(S_1S_4 + S_2S_3)$ (Scheme 2).

The experimental susceptibility data $\chi_M(T)$ were analyzed using a two-component fit function. The contribution due to the spin magnetic moments of the Ni_4 complexes was calculated using the spin Hamiltonian $\hat{H}_{spin} = \hat{H}_J + \hat{H}_{Zeeman} + \hat{H}_{aniso}$, with $\hat{H}_{Zeeman} = g\mu_B B\Sigma S_{z,I}$ and $\hat{H}_{aniso} = D\Sigma(S_{z,I}^2 - S_I(S_I + 1)/3)$ being the Zeeman and single-ion anisotropy terms, respectively. Furthermore a temperature-independent contribution (TIP) arising from spin−orbit coupling was added for **1b**. To reduce the total number of free parameters in the data analysis, we neglected the Curie tail at low temperatures that probably results from some residual paramagnetic impurity. Hence the data were analyzed only above temperatures T_{min} given in Table 3.

The magnetic susceptibility data for **1c** show a strong (field-independent) low temperature increase starting at temperatures close to 50 K. No reasonable modeling for this behavior could be obtained thus far. Results of the magnetic data analyses for complexes **1a**,**b**,**d**,**e** as well as **2a**,**b** are compiled in Table 2. Absolute numbers should be treated with care due to the large number of variables. For a better comparison of the magnetic exchange couplings the *g* factor has been fixed to 2.15 in the final analysis for all complexes. It is beyond doubt that one strong antiferromagnetic and one strong ferromagnetic coupling are found for all type **1** complexes. For the third interaction J_C a much smaller ferromagnetic coupling of ~10 cm^{-1} is found. Alternative models with, e.g., two antiferromagnetic and one ferromagnetic interactions gave a clearly worse fit. For type **2** complexes the data analyses gave a significantly reduced antiferromagnetic interaction J_A and much larger value for the single ion anisotropy *D*. Since the latter appears to be unreasonably large, results for type **2a**,**b** should only be interpreted with care. The strong ferromagnetic interaction J_B is almost the same in type **1** and **2** complexes. For J_C small values are found, either weakly positive and negative. It should be noted that due to the symmetry of the Hamiltonian the individual interactions J_A, J_B, and J_C are not unambiguously assigned to the topological *J* values in Scheme 2.

Discussion

To interpret the magnetic parameters determined for the various complexes, it appears reasonable to first consider separately the individual fragments of the tetranuclear framework. Ni1 and Ni2 (as well as Ni3 and Ni4) are spanned by the pyrazolate and by an *end-to-end* azide (as part of the central μ_4-azide), corresponding to J_1 in Scheme 2. A number of dinuclear nickel(II) complexes with only a single μ-1,3-azido bridge have been characterized magnetically.[20] Two geometric parameters, the angles Ni−N−N and the dihedral angle φ along the azide ligand, are often considered for magnetostructural correlations.[8,21] For a Ni−NNN−Ni torsion angle of $\varphi = 180°$, the antiferromagnetic coupling is predicted to have a maximum at Ni−N−N angles around 108° and to decrease at larger angles. On the other hand, for all Ni−N−N angles the maximum coupling is expected for a torsion of 180° (or 0°). However, the effect of torsion should be less pronounced than the effect of bond angle. In the absence of any constraining ligand scaffold, Ni−N−N angles in dinuclear complexes or 1D extended systems with one μ-1,3-azido bridge tend to lie in the range 115−145° with $\varphi = 140-180°$, resulting in *J* values in the range −17 to −100 cm^{-1}.[8,22] Particularly strong antiferromagnetic coupling of around −100 cm^{-1} has been observed for some 1D chain complexes with a *trans*-{Ni−(μ-1,3-N_3)−Ni} motif featuring acute Ni−N−N angles (120.9 or 115.6/116.8°, respectively) and a large φ (180 or 175.5°, respectively)[8,23] or in a dinickel(II) complex with extremely obtuse Ni−N−N angles of 109.9°.[24] In the case of all structurally characterized type **1** complexes, angles Ni−N−N for the μ_4-azide are found in the range 115.6−121.7°, and torsion angles Ni1−NNN−Ni2 as well as Ni3−NNN−Ni4 are close to zero (0.1−8.9°). A large antiferromagnetic *intra*dimer coupling in the order of −100 cm^{-1} can thus be anticipated for **1a**−

(20) (a) Pierpont, C. G.; Hendrickson, D. N.; Duggan, D. M.; Wagner, F.; Barefield, E. K. *Inorg. Chem.* **1975**, *14*, 604−610. (b) Wagner, F.; Mocella, M. T.; D'Aniello, M. J. J.; Wang, A. H. J.; Barefield, E. K. *J. Am. Chem. Soc.* **1974**, *96*, 2625−2627. (c) McLachlan, G. A.; Fallon, G. D.; Martin, R. L.; Moubaraki, B.; Murray, K. S.; Spiccia, L. *Inorg. Chem.* **1994**, *33*, 4663−4668. (d) Fabbrizzi, L.; Pallavicini, P.; Parodi, L.; Perotti, A.; Sardone, N.; Taglietti, A. *Inorg. Chim. Acta* **1996**, *244*, 7−9. (e) Escuer, A.; Harding, C. J.; Dussart, Y.; Nelson, J.; McKee, V.; Vicente, R. *J. Chem. Soc., Dalton Trans.* **1999**, 223−228. (f) Zhang, Z.-H.; Bu, X.-H.; Ma, Z.-H.; Bu, W.-M.; Tang, Y.; Zaho, Q.-H. *Polyhedron* **2000**, *19*, 1559−1566.

(21) de Biani, F. F.; Ruiz, E.; Cano, J.; Novoa, J. J.; Alvarez, S. *Inorg. Chem.* **2000**, *39*, 3221−3229.

(22) Meyer, F.; Kozlowski, H. In *Comprehensive Coordination Chemistry II*; McCleverty, J. A., Meyer, T. J., Eds.; Pergamon: Elmsford, NY, 2004; Vol. 6, pp 247−554.

(23) Vicente, R.; Escuer, A.; Ribas, J.; El Fallah, M. S.; Solans, X.; Font-Bardia, M. *Inorg. Chem.* **1995**, *34*, 1278−1281.

(24) Hausmann, J.; Klingele, M. H.; Lozan, V.; Steinfeld, G.; Siebert, D.; Journaux, Y.; Girerd, J. J.; Kersting, B. *Chem.−Eur. J.* **2004**, *10*, 1716−1728.

Table 3. Magnetic Parameters for the Complexes[a]

complex	J_A (cm^{-1})	J_B (cm^{-1})	J_C (cm^{-1})	g(fixed)	D (cm^{-1})	TIP (cm^3/mol)	T_{min}
1a	−110	+106	+2	2.15	−1	0	30
1b	−111	+51	+9	2.15	1	0.002 (fixed)	50
1d	−133	+129	+26	2.15	0	0	55
1e	−111	+86	+5	2.15	10	0	60
2a	−39	+98	−12	2.15	−46	0	20
2b	−50	+66	+7	2.15	−35	0	20

[a] Uncertainties for J values are in the order of 7−10 cm^{-1}.

e, in accordance with experimental findings. Hence, J_A in Table 3 is assigned to the intradimer coupling constant J_1 in Scheme 2 (some contribution from the pyrazolate is certainly present, but it is likely that the azide provides the dominant exchange pathway[13]). *Inter*dimer torsion angles of the *end-to-end* linkages Ni1−NNN−Ni4 and Ni2−NNN−Ni3 involving the μ_4-azide (J_3 in Scheme 2), however, are found in the range 102.7−119.7° for all type **1** complexes, that is, close to an orthogonal orientation. The antiferromagnetic contribution is likely to become negligible for this particular situation, and some ferromagnetic interaction might be possible for J_3. Very few examples of ferromagnetically coupled nickel(II) systems with μ-1,3-azido bridges have hitherto been discovered.[25−27] One is a dinuclear complex of a cryptate ligand that enforces unusual quasi-linearity of the central Ni−NNN−Ni unit (Ni−N−N angles close to 165°),[26] while the others are 1D compounds[25] or a Ni_4 complex[27] that exhibit appropriate Ni−NNN−Ni torsion angles (110.4, 106.8, 75.7, or 76.4°, respectively). In the latter cases, positive J values in the range +13.5 to +6.9 cm^{-1} have been attributed to quasi-orthogonality between the magnetic metal orbitals and the relevant azide p orbitals, which causes minimal overlap integrals through the bridge and hence a vanishing antiferromagnetic exchange contribution.[25] In view of the values for J_C obtained from the present magnetic data analysis (Table 3), the ferromagnetic diagonal interdimer interaction (J_3) in type **1** complexes apparently is of similar magnitude to those of previously reported compounds with a μ-1,3 azido bridge.

Dinuclear nickel(II) complexes with two *end-on* azido bridges and a {Ni(μ-1,1-N_3)$_2$Ni} central core generally feature Ni−N−Ni angles θ in the narrow range 101−105° and J values between +27 and +73 cm^{-1}.[8,22] DFT calculations suggested a clear correlation between the exchange coupling and θ, with the interaction predicted to be ferromagnetic for all the range of θ angles explored.[28] For the {Ni(μ-1,1-N_3)$_2$Ni} core, a maximum is expected at $\theta \approx 104°$. On the other hand, the out-of-plane displacement of the azide should only have a minor influence. The Ni1−N9−Ni3 and Ni2−N11−Ni4 angles involving the μ_4-azide in type **1** complexes are very acute in the range 91.0−93.7°, while the Ni1−N12−Ni3 and Ni2−N15−Ni4 angles for the μ-1,1-azide are a little wider (96.5−97.9°). Since the carboxylate is not expected to contribute considerably to the interdimer coupling J_2, a significant ferromagnetic interaction can be anticipated. In view of these considerations, we tentatively assign the larger ferromagnetic coupling J_B to the short edges of the Ni_4 rectangle (J_2 in Scheme 2) and the smaller ferromagnetic interaction J_C to the diagonal interdimer exchange (J_3 in Scheme 2). It is interesting to note that the combination of one antiferromagnetic and two ferromagnetic interactions in type **1** complexes reveals some degree of frustration, introduced by the smaller ferromagnetic interaction J_3.

In contrast to the situation in type **1** complexes, the molecular structure of **2b** reveals considerable torsion along the *end-to-end* linkages of the μ_4-azide, 52.7° for Ni1−NNN−Ni2 and 52.8° for Ni3−NNN−Ni4 (while Ni−N−N angles are in the same range as above, 117.2−118.7°). Consequently, a significantly smaller intradimer antiferromagnetic coupling J_1 is expected, in accordance with experimental findings for J_A. Due to the double carboxylate bridges, angles Ni1−N9−Ni3 (124.4(2)°) and Ni2−N11−Ni4 (124.1(2)°) are much wider for **2b** than for type **1** complexes. Despite this and the absence of the μ-1,1 azide, however, ferromagnetic coupling J_B is of the same order of magnitude for **2a**,**b** and type **1** compounds. Ferromagnetic exchange has recently been reported for a μ-1,1-azido-bridgednickel(II) dimer with a very large θ value of 129.3°, corroborating that a μ-1,1-azido group may be considered an almost universal ferromagnetic coupler.[29] Torsion angles along the diagonal *end-to-end* linkages of the μ_4-azide are 126.6° (Ni1−NNN−Ni4) or 127.9° (Ni2−NNN−Ni3) for **2b**. This might again be a situation where ferro- and antiferromagnetic contributions largely compensate, since small numbers J_C are determined for both **2a**,**b**. It should be emphasized though that all magneto−structural correlations for type **2** complexes discussed above need to be qualified, because good X-ray crystallographic results are available for only a single compound and the theoretical fits to the experimental magnetic data are of moderate quality (as can be seen from calculated D values which are unreasonably large). The synthesis of further examples of this intriguing class of complexes and a more comprehensive magnetic analysis is certainly warranted.

(25) (a) Hong, C. S.; Do, Y. *Angew. Chem., Int. Ed.* **1999**, *38*, 193−195. (b) Montfort, M.; Resino, I.; Ribas, J.; Stoeckli-Evans, H. *Angew. Chem., Int. Ed.* **2000**, *39*, 191−193. (c) Hong, C. S.; Koo, J.; Son, S.-K.; Lee, Y. S.; Kim, Y.-S.; Do, Y. *Chem.—Eur. J.* **2001**, *7*, 4243−4252. (d) Mukherjee, P. S.; Dalai, S.; Zangrando, E.; Lloret, F.; Chaudhuri, N. R. *Chem. Commun.* **2001**, 1444−1445.

(26) Escuer, A.; Harding, C. J.; Dussart, Y.; Nelson, J.; McKee, V.; Vicente, R. *J. Chem. Soc., Dalton Trans.* **1999**, 223−227.

(27) Kersting, B.; Steinfeld, G.; Siebert, D. *Chem.—Eur. J.* **2001**, *7*, 4253−4258.

(28) Ruiz, E.; Cano, J.; Alvarez, S.; Alemany, P. *J. Am. Chem. Soc.* **1998**, *120*, 11122−11129.

(29) Mialane, P.; Dolbecq, A.; Rivière, E.; Marrot, J.; Sécheresse, F. *Angew. Chem., Int. Ed.* **2004**, *43*, 2274−2277.

Conclusions

A whole series of unusual Ni_4 complexes composed of two pyrazolate-based dinuclear building blocks has been prepared and fully characterized. All new complexes feature an unprecedented central μ_4-1,1,3,3-azido ligand, which apparently is quite flexible with respect to its coordination geometry and which is capable of adapting to different arrangements of the four metal ions. Two classes of complexes with considerably different Ni−N_{azide}−Ni angles and Ni−NNN−Ni torsions for the μ_4-azide are found, which is reflected by the distinct IR-spectroscopic signatures and different magnetic properties. All compounds are shown to have an $S = 0$ ground state, but individual *intra*dimer and *inter*dimer coupling constants differ depending on the geometrical details of the Ni_4 core, where the torsion angles along the central μ_4-azide appears to play a major role. It is concluded that magneto−structural correlations for the novel μ_4-azido linkage parallel those described for the more common μ-1,1- and μ-1,3-azido bridges. Several features remain to be clarified though, such as the unique asymmetry of the central μ_4-azide in **1a** and subtle differences in the magnetic properties of the various species. Experiments aimed at extending the number of complexes with μ_4-1,1,3,3-azido ligands are in progress.

Experimental section

General Methods. Manipulations were carried out under an atmosphere of nitrogen by using standard Schlenk techniques. Solvents were dried by established processes. Na_2CO_3 was dried by heating to 100 °C for 6 h under vacuum. 3,5-Bis(chloromethyl)-1-(tetrahydropyran-2-yl)-1*H*-pyrazole,[30] [2-(ethylsulfanyl)ethyl]-methylamine,[31] bis[2-(methylsulfanyl)ethyl]amine,[32] and bis[2-(ethylsulfanyl)ethyl]amine[18] were synthesized according to the reported methods. The bis(alkylsulfanylethyl)amines have been reported previously and were synthesized in a similar fashion—only spectral data are reported here.[18,31,32,33] All other chemicals were purchased from commercial sources and used as received. Microanalyses were performed by the Analytisches Labor des Anorganisch-Chemischen Instituts der Universität Göttingen. UV/vis spectra were measured with an Analytik Jena Specord S 100, IR spectra with a Digilab Excalibur (recorded as KBr pellets), mass spectra with a Finnigan MAT 8200 (EI-MS), a Finnigan MAT 95 (FAB-MS), or a Finnigan MAT LCQ (ESI-MS), and NMR spectra at 300 K on a Bruker Avance 500 at 500.13 (^{1}H) and 125.77 (^{13}C) MHz (residual solvent signal as chemical shift reference; $CDCl_3$, $\delta_H = 7.27$, $\delta_C = 77.0$). The susceptibility measurements were carried out with a Quantum-Design-MPMS 5S SQUID magnetometer in the range from 300 to 2 K. The powdered samples were contained in a gel bucket and fixed in a nonmagnetic sample holder. Each raw data file for the measured magnetic moment was corrected for the diamagnetic contribution of the sample holder and the gel bucket. The molar susceptibility data were corrected for diamagnetism by using the Pascal constants and the increment method according to Haberditzl.[34]

Caution! *Although no problems were encountered in this work, transition metal perchlorate and azide complexes are potentially explosive and should be handled with proper precautions.*

Bis[2-(1-methyl-ethylsulfanyl)ethyl]amine.[33] A solution of bis-(2-chloroethyl)amine hydrochloride (17.7 g, 100 mmol) in ethanol (200 cm^3) was added to a solution of NaOH (12 g, 300 mmol) and 1-(methylethyl)ethanethiol (22.8 g, 300 mmol) in ethanol (300 cm^3) at 0 °C. The mixture was stirred for 2 h and filtered and the filtrate evaporated to dryness.The residue was taken up in Et_2O and filtered again. The solvent was removed by evaporation under reduced pressure and the remaining residue distilled to give 37.2 g (84%) of a colorless, viscous liquid. Bp: 145 °C/10 mbar. ^{1}H NMR ($CDCl_3$): $\delta = 1.26$ (d, J(HH) = 6.7 Hz, CH*CH*$_3$, 12H), 1.94 (s, NH, 1H), 2.68 (t, J(HH) = 6.5 Hz, SCH_2, 4H), 2.82 (t, J(HH) = 6.5 Hz, NCH_2, 4H), 2.93 (sept, J(HH) = 6.7 Hz, *CH*CH_3, 2H). ^{13}C NMR ($CDCl_3$): $\delta = 22.8$ (CH*CH*$_3$), 30.1 (SCH_2), 33.9 (NCH_2), 48.0 (*CH*CH_3). MS (EI): m/z (%) = 221 (5), $[M]^+$, 132 (70), $[M - CH_2S^iPr]^+$, 103 (100), $[M - HN(CH_2)_2S^iPr]^+$. Anal. Calcd for $C_{10}H_{23}NS_2$ ($M_r = 221.4$): C, 54.24; H, 10.47; N, 6.33. Found: C, 54.48; H, 10.43; N, 6.48.

***N*-Methyl-[(2-ethylsulfanyl)ethyl]amine.** A solution of (2-chloroethyl)methylamine (18.7 g, 200 mmol) in ethanol (200 cm^3) was added to a solution of NaOH (8.4 g, 210 mmol) and ethanthiol (24.8 g, 400 mmol) in ethanol (300 cm^3) at 0 °C. After the mixture was stirred for 2 h, the suspension was filtered and the filtrate evaporated to dryness. The residue was taken up in Et_2O and filtered again. After evaporation of the solvent under reduced pressure, the residue was distilled and yielded 15.8 g (66%) of a colorless liquid, bp 70 °C/10 mbar. ^{1}H NMR ($CDCl_3$): $\delta = 0.80$ (t, J(HH) = 7.3 Hz, CH_2CH_3, 3H), 1.45 (s, NH, 1H), 2.05 (s, NCH_3, 3H), 2.15 (q, J(HH) = 7.3 Hz, CH_2CH_3, 2H), 2.27−2.38 (m, SCH_2, 2H), 2.47−2.58 (m, NCH_2, 2H). ^{13}C NMR ($CDCl_3$): $\delta = 14.2$ (CH_2CH_3), 25.1 (NCH_3), 31.0 (CH_2), 35.4 (CH_2), 50.0 (CH_2). MS (EI): m/z (%) = 119 (10), $[M]^+$, 44 (100), $[M - CH_2SC_2H_5]^+$. Anal. Calcd for $C_5H_{13}NS$ ($M_r = 119.2$): C, 50.37; H, 10.99; N, 11.75. Found: C, 49.69; H, 10.90; N, 12.37.

General Synthetic Procedure for the Pyrazolate-Based Ligands. A mixture of 42 g (400 mmol) of predried Na_2CO_3, 400 mL of dry acetonitrile, 10 g (40 mmol) of 3,5-bis(chloromethyl)-1-(tetrahydropyran-2-yl)-1*H*-pyrazole, and 90 mmol of the respective amine was stirred and heated to reflux for 24 h. After filtration, all volatile material was removed under reduced pressure. The residue was taken up in ethanol (50 mL), treated with ethanolic hydrochloric acid, and stirred overnight. Addition of diethyl ether caused precipitation of the hydrochloride salt of HL_1, HL_2, HL_3, or HL_4, respectively. This was separated and treated with aqueous NaOH (4 M), and the aqueous solution was extracted several times with dichloromethane. The combined organic phases were dried with $MgSO_4$ and filtered. After removal of the solvent under reduced pressure, HL_1 (12.1 g, 72%), HL_2 (14.5 g, 76%), HL_3 (14.9 g, 70%), and HL_4 (7.9 g, 60%) were obtained as slightly yellow, viscous liquids.

3,5-Bis{*N*,*N*-bis[2-(methylsulfanyl)ethyl]aminomethyl}-1*H*-pyrazole (HL^1). ^{1}H NMR ($CDCl_3$): $\delta = 1.85$ (s, SCH_3, 12H), 2.39 (t, J(HH) = 6.5 Hz, SCH_2, 8H), 2.53 (t, NCH_2, J(HH) = 6.5 Hz,

(30) (a) Schenck, T. G.; Downes, J. M.; Milne, C. R. C.; Mackenzie, P. B.; Boucher, T. G.; Whelan, J.; Bosnich, B. *Inorg. Chem.* **1985**, *24*, 2334−2337. (b) Röder, J. C.; Meyer, F.; Pritzkow, H. *Organometallics* **2001**, *20*, 811−817.

(31) (a) Bannard, R. A. B.; Parkkari, J. H.; Coleman, I. W. *Can. J. Chem.* **1962**, *40*, 1909−1916. (b) Parkkari, J. H.; Bannard, R. A. B.; Coleman, I. W. *Can. J. Chem.* **1965**, *43*, 3119−3128.

(32) McGuinness, D. S.; Wasserscheid, P.; Keim, W.; Morgan, D.; Dixon, J. T.; Bollmann, A.; Maumela, H.; Hess, F.; Englert, U. *J. Am. Chem. Soc.* **2003**, *125*, 5272−5273.

(33) Le, X.-Y.; Shi, J.-E. *Wuji Huaxue Xuebao* **1999**, *15*, 128−131.

(34) (a) Haberditzl, W. *Angew. Chem.* **1966**, *78*, 277−288; *Angew. Chem., Int. Ed. Engl.* **1966**, *5*, 288−298. (b) Haberditzl, W. *Magnetochemistry*; Akademie-Verlag: Berlin, 1968.

8H), 3.52 (s, pzCH_2, 4H), 5.89 (s, pz-*H*,[4] 1H), 10.65 (br, NH, 1H). ^{13}C NMR ($CDCl_3$): δ = 15.1 (SCH_3), 31.4 (SCH_2), 49.7 (NCH_2), 52.6 (pzCH_2), 103.5 (pz-C^4), 149.0 (br, pz-$C^{3,5}$). MS (EI): *m*/*z* (%) = 361 (100), $[M - CH_2SCH_3]^+$, 258 (25), $[M - N(C_2H_4SCH_3)_2]^+$, 75 (60), $[CH_3(CH_2)_2]^+$. Anal. Calcd for $C_{17}H_{34}N_4S_4$ (M_r = 422.7): C, 48.30; H, 8.11; N, 13.25. Found: C, 48.48; H, 8.07; N, 13.62.

3,5-Bis{*N*,*N*-bis[2-(ethylsulfanyl)ethyl]aminomethyl}-1*H*-pyrazole (HL^2). ^{1}H NMR ($CDCl_3$): δ = 1.10 (t, *J*(HH) = 7.3 Hz, CH_2CH_3, 12H), 2.35 (q, ^{3}*J*(HH) = 7.3 Hz, CH_2CH_3, 8H), 2.50−2.75 (m, NCH_2CH_2S, 16H), 3.56 (s, pzCH_2, 4H), 5.92 (s, pz-*H*,[4] 1H). ^{13}C NMR ($CDCl_3$): δ = 14.7 (CH_2CH_3), 26.0 (SCH_2), 29.4 (NCH_2), 53.65 (pzCH_2), 103.3 (pz-C^4), 145.5 (pz-$C^{3,5}$). MS (EI): *m*/*z* (%) = 403 (100), $[M - CH_2SC_2H_5]^+$, 286 (25), $[M - N((CH_2)_2SC_2H_5)_2]^+$, 89 (70), $[C_2H_5S(CH_2)_2]^+$. Anal. Calcd for $C_{21}H_{42}N_4S_4$ (M_r = 478.9): C, 52.67; H, 8.84; N, 11.70. Found: C, 52.95; H, 8.72; N, 11.97.

3,5-Bis{*N*,*N*-bis[2-(1-methylethylsulfanyl)ethyl]aminomethyl}-1*H*-pyrazole (HL^3). ^{1}H NMR ($CDCl_3$): δ = 1.20 (d, *J*(HH) = 6.7 Hz, $CHCH_3$, 24H), 2.51−2.65 (m, NCH_2CH_2S, 16H), 2.80 (sept, *J*(HH) = 6.7 Hz, $CHCH_3$, 4H), 3.62 (s, pz-CH_2, 4H), 5.95 (s, pz-*H*,[4] 1H). ^{13}C NMR ($CDCl_3$): δ = 23.3 ($CHCH_3$), 28.27 (SCH_2), 34.7 (NCH_2), 50.2 ($CHCH_3$), 53.7 (pzCH_2), 103.3 (pz-C^4), 145.7 (br, pz-$C^{3,5}$). MS (EI): *m*/*z* (%) = 534 (2), $[M]^+$, 445 (100), $[M - C_3H_7SCH_2]^+$, 314 (10), $[M - N(C_2H_5SC_3H_7^i)_2]^+$, 103 (60), $[C_3H_7^iS(CH_2)_2]^+$. Anal. Calcd for $C_{25}H_{50}N_4S_4$ (M_r = 535.0): C, 56.13; H, 9.42; N, 10.47. Found: C, 55.96; H, 9.38; N, 10.86.

3,5-Bis[*N*-methyl-*N*-(2-ethylsulfanyl)ethyl]aminomethyl-1*H*-pyrazole (HL^4). ^{1}H NMR ($CDCl_3$): δ = 1.12 (t, *J*(HH) = 7.4 Hz, CH_2CH_3, 3H), 2.19 (s, NCH_3, 3H), 2.40 (q, *J*(HH) = 7.4 Hz, CH_2CH_3, 2H), 2.52 (s, NCH_2CH_2S, 4H), 3.52 (s, pzCH_2, 4H), 6.01 (s, pz-H,[4] 1H). ^{13}C NMR ($CDCl_3$): δ = 14.5 (CH_2CH_3), 25.7 (NCH_3), 28.8 (SCH_2), 41.9 (SCH_2), 53.4 (pzCH_2), 56.2 ($CHCH_3$), 103.5 (pz-C^4), 145.0 (pz-$C^{3,5}$). MS (EI): *m*/*z* (%) = 330 (2), $[M]^+$, 329 (4), $[M - H]^+$, 269 (10), $[M - SC_2H_5]^+$, 255 (100), $[M - CH_2SC_2H_5]^+$, 212 (60), $[M - CH_3N(CH_2)_2SC_2H_5]^+$, 89 (45), $[(CH_2)_2SC_2H_5]^+$. Anal. Calcd for $C_{15}H_{30}N_4S_2$ (M_r = 330.6): C, 54.50; H, 9.15; N, 16.95. Found: C, 54.19; H, 8.97; N, 17.64.

Synthesis of $[(L^4)_2Ni_4(N_3)_3(O_2CMe)_2](ClO_4)\cdot$acetone (1a). A solution of HL^4 (198 mg, 0.60 mmol) in methanol (20 mL) was treated with 1 equiv of KO^{t}Bu (71 mg, 0.60 mmol), 1.5 equiv of $Ni(ClO_4)_2\cdot 6H_2O$ (329 mg, 0.90 mmol), and 0.5 equiv of $Ni(O_2CMe)_2\cdot 4H_2O$ (75 mg, 0.30 mmol). After the mixture was stirred for 1 h at room temperature, the solution was evaporated to dryness and the residue was taken up in acetone (25 mL). NaN_3 (59 mg, 0.90 mmol) was added, and the reaction mixture was stirred for further 12 h. The precipitate was separated by filtration, and the resulting green solution was layered with light petroleum ether (boiling range 40−60 °C, 75 mL) to obtain green crystals of the product **1a** (208 mg, 56%). IR (KBr, cm^{-1}): 2081 (vs), 2070 (vs), 2052 (s) [$\nu(N_3^-)$]; 1705 (w) [$\nu(C{=}O)_{acetone}$]; 1584 (s) [$\nu(C{=}O)_{acetate}$]; 1122 (s), 1109 (s), 1090 (s) [$\nu(ClO_4^-)$]. MS (FAB+): *m*/*z* (%) = 1136 (74), $[(L^4)_2Ni_4(N_3)_3(O_2CMe)_2]^+$, 563 (72), $[L^4Ni_2(O_2CMe)_2]^+$, 546 (100), $[L^4Ni_2(N_3)(O_2CMe)]^+$, 504 (5), $[L^4Ni_2(O_2CMe)]^+$, 445 (12), $[L^4Ni_2]^+$. Anal. Calcd for $C_{34}H_{64}N_{17}Ni_4O_8S_4Cl\cdot C_3H_6O$ (M_r = 1295.6): C, 34.30; H, 5.47; N, 18.40. Found: C, 34.30; H, 5.40; N, 18.15.

Synthesis of $[(L^4)_2Ni_4(N_3)_3(O_2CPh)_2](ClO_4)\cdot NaClO_4\cdot$2 acetone$\cdot H_2O$ (1b). A solution of HL^4 (198 mg, 0.60 mmol) in methanol (20 mL) was treated with 1 equiv of KO^{t}Bu (71 mg, 0.60 mmol) and 2 equiv of $Ni(ClO_4)_2\cdot 6H_2O$ (439 mg, 1.20 mmol). After the mixture was stirred for 1 h at room temperature, the solution was evaporated to dryness and the residue was taken up in acetone (25 mL). Na(O_2CPh) (86 mg, 0.60 mmol) and NaN_3 (59 mg, 0.90 mmol) were added, and the reaction mixture was stirred for further 24 h. The precipitate was separated by filtration, and the resulting green solution was layered with light petroleum ether (boiling range 40−60 °C, 75 mL) to obtain green crystals of the product **1b** (117 mg, 24%). IR (KBr, cm^{-1}): 3425 (m, br) [ν(OH)]; 2080 (vs), 2073 (vs), 2044 (s) [$\nu(N_3^-)$]; 1708 (w) [$\nu(C{=}O)_{acetone}$]; 1601 (s), 1567 (s) [$\nu(C{=}O)_{benzoate}$]; 1121 (s), 1107 (s), 1091 (s) [$\nu(ClO_4^-)$]. MS (FAB+): *m*/*z* (%) = 1260 (92), $[(L^4)_2Ni_4(N_3)_3(O_2CPh)_2]^+$, 687 (68), $[L^4Ni_2(O_2CPh)_2]^+$, 608 (100), $[L^4Ni_2(N_3)(O_2CPh)]^+$, 507 (15), $[L^4Ni(O_2CPh)]^+$. Anal. Calcd for $C_{44}H_{68}N_{17}NaNi_4O_{12}S_4Cl_2\cdot C_3H_6O\cdot H_2O$ (M_r = 1560.1): C, 36.18; H, 4.91; N, 15.26. Found: C, 36.37; H, 4.87; N, 14.82.

Synthesis of $[(L^2)_2Ni_4(N_3)_3(O_2CMe)_2](ClO_4)$ (1c). The synthesis was carried out in analogy to the procedure described for **1a,** starting from HL^2 (287 mg, 0.60 mmol). An amount of 175 mg (38%) of the product **1c** was obtained. IR (KBr, cm^{-1}): 2079 (vs), 2074 (vs), 2043 (m) [$\nu(N_3^-)$]; 1587 (s) [$\nu(C{=}O)_{acetate}$]; 1122 (m), 1096 (s) [$\nu(ClO_4^-)$]. MS (FAB+): *m*/*z* (%) = 1434 (4), $[(L^2)_2Ni_4(N_3)_3(O_2CMe)_2]^+$, 1375 (5), $[(L^2)_2Ni_4(N_3)_3(O_2CMe)]^+$, 696 (100), $[L^2Ni_2(N_3)(O_2CMe)]^+$, 635 (20), $[L^2Ni_2(N_3)]^+$, 536 (12), $[L^2Ni]^+$. Anal. Calcd for $C_{46}H_{88}N_{17}Ni_4O_8S_8Cl$ (M_r = 1534.1): C, 36.02; H, 5.78; N, 15.52. Found: C, 35.42; H, 5.73; N, 15.07.

Synthesis of $[(L^3)_2Ni_4(N_3)_3(O_2CMe)_2](ClO_4)$ (1d). The synthesis is similar to the procedure described for **1a,** starting from HL^3 (321 mg, 0.60 mmol). An amount of 112 mg (22%) of the product **1d** was obtained. IR (KBr, cm^{-1}): 3425 (m, br) [ν(OH)]; 2082 (vs), 2073 (vs), 2044 (m) [$\nu(N_3^-)$]; 1587 (s) [$\nu(C{=}O)_{acetate}$]; 1122 (m), 1095 (s) [$\nu(ClO_4^-)$]. MS (FAB+): *m*/*z* (%) = 1546 (10), $[(L^3)_2Ni_4(N_3)_3(O_2CMe)_2]^+$, 769 (24), $[L^3Ni_2(O_2CMe)_2]^+$, 750 (100), $[L^3Ni_2(N_3)(O_2CMe)]^+$, 735 (20), $[L^3Ni_2(N_3)_2]^+$, 693 (7), $[L^3Ni\ N_3]^+$, 650 (12), $[L^3Ni]^+$. Anal. Calcd for $C_{54}H_{104}N_{17}Ni_4O_8S_8Cl\cdot 2H_2O$ (M_r = 1682.3): C, 38.55; H, 6.47; N, 14.15. Found: C, 38.05; H, 6.13; N, 13.58.

Synthesis of $[(L^3)_2Ni_4(N_3)_3(O_2CAda)_2](ClO_4)\cdot$acetone (1e). The synthesis is similar to the procedure described for **1b,** starting from HL^3 (321 mg, 0.60 mmol). K(O_2CAda) was prepared in situ from HO_2CAda (108 mg, 0.60 mmol) and KO^{t}Bu (71 mg, 0.60 mmol). An amount of 135 mg (23%) of the product **1e** was obtained. IR (KBr, cm^{-1}): 2081 (vs), 2072 (vs), 2045 (m) [$\nu(N_3^-)$]; 1705 [w, $\nu(C{=}O)_{acetone}$]; 1567 (s) [$\nu(C{=}O)_{ada}$]; 1121 (m), 1096 (s) [$\nu(ClO_4^-)$]. MS (FAB+): *m*/*z* (%) = 1787 (12), $[(L^3)_2Ni_4(N_3)_3(O_2CAda)_2]^+$, 1010 (16), $[L^3Ni_2(O_2CAda)_2]^+$, 872 (100), $[L^3Ni_2(N_3)(O_2CAda)]^+$, 735 (12), $[L^3Ni(N_3)_2]^+$, 693 (8), $[L^3Ni(N_3)]^+$. Anal. Calcd for $C_{72}H_{128}N_{17}Ni_4S_8O_8Cl\cdot C_3H_6O$ (M_r = 1944.7): C, 46.32; H, 6.95; N, 12.24. Found: C, 46.19; H, 6.93; N, 11.96.

Synthesis of $[(L^1)_2Ni_4(N_3)(O_2CAda)_4](ClO_4)$ (2a). A solution of HL^1 (254 mg, 0.60 mmol) in methanol (20 mL) was treated with 1 equiv of KO^{t}Bu (71 mg, 0.60 mmol) and 2 equiv of $Ni(ClO_4)_2\cdot 6H_2O$ (439 mg, 1.20 mmol). After the mixture was stirred for 1 h at room temperature, the blue solution was treated with NaN_3 (59 mg, 0.90 mmol), whereupon the color changes to green. The green reaction mixture was carefully layered with methanol (20 mL), and then a solution of KO_2CAda (131 mg, 0.60 mmol) in methanol (20 mL) was added on top as a third layer. After standing for a couple of days, green crystals were obtained in the diffusion zone. Purification was achieved by layering a dichlormethane (20 mL) solution of the green crystals with light petroleum ether (boiling range 40−60 °C, 80 mL), which leads to the pure product **2a** (27 mg, 5%). IR (KBr, cm^{-1}): 2128 (s) [$\nu(N_3^-)$]; 2054 (m); 1585 (vs) [$\nu(C{=}O)_{ada}$]; 1142 (vs), 1107 (vs), 1089 (vs) [$\nu(ClO_4^-)$]. MS (ESI+, MeCN): *m*/*z* (%) = 1835 (100), $[(L^1)_2Ni_4(N_3)(O_2CAda)_4]^+$. MS (FAB+): *m*/*z* (%) = 1835 (12), $[(L^1)_2Ni_4(N_3)(O_2CAda)_4]^+$, 897 (45), $[L^1Ni_2(O_2CAda)_2]^+$, 758 (15), $[L^1Ni_2(O_2CAda)(N_3)]^+$. Anal.

Table 4. Crystal Data and Refinement Details for Complexes **1a,b,e** and **2b**

	1a	**1b**	**1e**	**2b**
formula	$C_{37}H_{70}ClN_{17}Ni_4O_9S_4$	$C_{50}H_{82}Cl_2N_{17}NaNi_4O_{15}S_4$	$C_{75}H_{134}N_{17}ClNi_4O_9S_8$	$C_{86}H_{142}N_{11}ClNi_4O_{12}S_8$
M_r	1295.63	1618.30	1944.76	2048.88
cryst size (mm^3)	0.35 × 0.35 × 0.30	0.30 × 0.15 × 0.15	0.50 × 0.35 × 0.30	0.30 × 0.10 × 0.09
cryst system	monoclinic	triclinic	triclinic	monoclinic
space group	$P2_1$	$P\bar{1}$	$P\bar{1}$	$P2_1$
a (Å)	12.6894(9)	11.3935(7)	14.679(2)	16.391(2)
b (Å)	19.330 (1)	14.8784(9)	16.571(2)	16.515(2)
c (Å)	22.324(2)	21.4752(13)	20.216(2)	18.416(2)
α (deg)	90	92.192(1)	101.178(3)	90
β (deg)	91.480(1)	91.540(1)	102.587(3)	103.902(3)
γ (deg)	90	107.582(1)	90.957(3)	90
V ($Å^3$)	5474.0(6)	3465.0(4)	4699.0(12)	4839.2(11)
ρ_{calcd} (g/cm^3)	1.572	1.551	1.374	1.406
Z	4	2	2	2
F(000)	2704	1684	2064	2176
temp (K)	103(2)	103(2)	297(2)	106(2)
hkl range	±18, ±28, 0−33	±16, ±22, 0−31	±20, ±23, 0−28	−20 to 19, −20 to 14, 0−23
2θ range (deg)	2.8−64.0	3.36−64.0	3.14−61.02	3.56−52.74
measd reflns	89 619	60 909	75 471	30 326
unique reflns	36 851 [R(int) = 0.0369]	23 457 [R(int) = 0.0426]	28 487 [R(int) = 0.0348]	14 795 [R(int) = 0.0568]
obsd reflns [$I > 2\sigma(I)$]	33 896	15 790	20 188	11 505
refined params	1339	1177	1146	1115
resid electron dens (e $Å^{-3}$)	2.67 and −1.40	1.94 and −1.63	1.39 and −0.68	1.04 and −0.57
R1 [$I > 2\sigma(I)$]	0.0658	0.0435	0.0559	0.0509
wR2 (all data)	0.1686	0.1184	0.1671	0.1346
GOF	1.109	1.030	1.077	1.036

Calcd for $C_{78}H_{126}N_{11}Ni_4S_8O_{12}Cl$ (M_r = 1936.7): C, 48.37; H, 6.58; N, 7.96. Found: C, 48.09; H, 6.72; N, 7.68.

Synthesis of $[(L^2)_2Ni_4(N_3)(O_2CAda)_4](ClO_4)$ (2b). A solution of HL^2 (287 mg, 0.60 mmol) in dichloromethane (20 mL) was treated with 1 equiv of KO^{t}Bu (71 mg, 0.60 mmol) and 2 equiv of $Ni(ClO_4)_2 \cdot 6H_2O$ (439 mg, 1.20 mmol). After the mixture was stirred for 1 h at room temperature, HO_2CAda (216 mg, 1.20 mmol), KO^{t}Bu (142 mg, 1.20 mmol), and NaN_3 (30 mg, 0.45 mmol) were added. The reaction mixture was stirred for further 24 h, and the precipitate was separated by filtration. The resulting green solution was layered with light petroleum ether (boiling range 40−60 °C, 75 mL) to obtain green crystals of the product **2b** (107 mg, 17%). IR (KBr, cm^{-1}): 2127 (s) [$\nu(N_3^-)$]; 2043 (m); 1582 (vs) [$\nu(C{=}O)_{ada}$]; 1144 (s), 1103 (vs), 1088 (vs) [$\nu(ClO_4^-)$]. MS (FAB+): m/z (%) = 1949 (5), $[(L^2)_2Ni_4(N_3)(O_2CAda)_4]^+$, 953 (100), $[L^2Ni_2(O_2CAda)_2]^+$, 816 (12), $[L^2Ni_2(N_3)(O_2CAda)]^+$. Anal. Calcd for $C_{86}H_{142}N_{11}Ni_4S_8O_{12}Cl$ (M_r = 2048.9): C, 50.41; H, 6.99; N, 7.52. Found: C, 50.13; H, 6.94; N, 7.57.

Analysis of Magnetic Data. Analysis of the magnetic susceptibility data using the spin Hamiltonian $\hat{H}_{spin} = \hat{H}_J + \hat{H}_{Zeeman} + \hat{H}_{aniso}$ (with $\hat{H}_{Zeeman} = g\mu_B B\Sigma S_{z,I}$ and $\hat{H}_{aniso} = D\Sigma(S_{z,I}^2 - S_I(S_I + 1)/3$ being the Zeeman and single-ion anisotropy terms, respectively) was performed by (i) numerically diagonalizing the Hamiltonian $\hat{H}_{spin}$ in the S_z basis of the $3^4 = 81$-dimensional Hilbert space by computer algebra, (ii) calculating the free energy A_{spin} and magnetization M for magnetic field orientations parallel and perpendicular to the z-axis, and (iii) fitting the sum of the spin magnetization $M = 1/3M_{||} + 2/3M_{\perp}$ (polycrystalline average) (and for **1b** a TIP) to the data using MATHEMATICA.

X-ray Crystallography. Data collection was carried out on a Bruker AXS CCD diffractometer using graphite-monochromated Mo Kα radiation (λ = 0.710 73 Å). Structures were solved by direct methods (SHELXS-97) and refined by full-matrix least-squares techniques based on F^2 (SHELXL-97).[35] Atomic coordinates and thermal parameters of the non-hydrogen atoms were refined in fully anisotropic models. Hydrogen atoms were either located in the difference Fourier map and refined isotropically or included using the riding model. X-ray data are compiled in Table 4.

Acknowledgment. We thank Fabian Heidrich-Meisner and Dr. Andreas Honecker (Institut für Theoretische Physik, TU Braunschweig) for substantial help creating the spin Hamiltonian matrix. Financial support by the DFG (Priority Program 1137 "Molecular Magnetism") and the Fonds der Chemischen Industrie is gratefully acknowledged.

Supporting Information Available: Crystallographic data, in CIF format, for **1a**,**b**,**e** and **2b**, ORTEP plots of **1a**,**b**,**e** and **2b** (Figures S1−S4), and χ_M and $\chi_M T$ vs T plots for **1a**,**c**,**e** and **2a** (Figures S5−S8). This material is available free of charge via the Internet at http://pubs.acs.org.

IC049251P

(35) Sheldrick, G. M. *SHELXS-97, Program for Crystal Structure Solution*; Universität Göttingen: Göttingen, Germany, 1997. Sheldrick, G. M. *SHELXL-97, Program for Crystal Structure Refinement*; Universität Göttingen: Göttingen, Germany, 1997.